Composition and function of integrin adhesions

Zuidema, A.C.

PEAK1 regulates colorectal cancer cell proliferation and polarity in a context-dependent manner

Alba Zuidema[1], Maaike Kreft[1], Martine Bierbooms[1], Lona Kroese[2], Ji-Ying Song[3], Sabine van der Poel[1], Sophie Verhoeven[1], Rahmen Bin Ali[2], Ivo Huijbers[2], Arnoud Sonnenberg[1].

[1] Division of Cell Biology, The Netherlands Cancer Institute, Amsterdam, The Netherlands;
[2] Mouse Clinic for Cancer and Aging research (MCCA) Transgenic Facility, The Netherlands Cancer Institute, Amsterdam, The Netherlands;
[3] Experimental Animal Pathology, The Netherlands Cancer Institute, Amsterdam, The Netherlands.

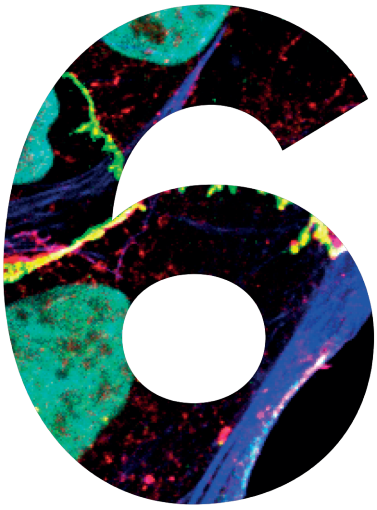

ABSTRACT

The scaffold protein PEAK1 acts downstream of integrin adhesion complexes and the EGF receptor to coordinate signaling events that control cell proliferation and cytoskeletal remodeling. PEAK1 was found to be more phosphorylated on Y635 in colorectal adenomas than carcinomas in a phosphoproteomic screen that was employed to identify potential drivers of the adenoma-to-carcinoma progression. In this study, the role of PEAK1 in CRC was investigated by deleting PEAK1 by CRISPR/Cas9 in different *in vitro* and *in vivo* models that mimic the stepwise pathogenesis of CRC. The data show that PEAK1 does not regulate the proliferation of SW480 and HT29 cells, nor does it regulate tumor development in CRC mouse models driven by oncogenic KRAS or loss of PTEN. However, PEAK1 does promote EGF-induced Caco-2 cell proliferation and regulates spheroid polarization and lumenization, possibly by regulating expression of Scribble. These data indicate that PEAK1 does not play a major role in CRC progression, although it might regulate cell polarity and growth during early adenoma formation.

INTRODUCTION

Colorectal cancer (CRC) is one of the most prevalent forms of cancer and the second most common cause of cancer-related deaths in the western world [1-3]. The disease begins with the formation of a benign adenoma, which can progress into an invasive cancer (carcinoma) and eventually become metastatic. Common events in the multi-step progression of CRC are mutational inactivation of tumor suppressor genes (*APC*, *PTEN*, *TP53*) and activation of oncogenes (*RAS*, *BRAF*, *PIK3CA*) [4-6]. Despite extensive knowledge of the genomic aberrations in CRC, it is still unclear how these affect the expression and activation status of proteins and signaling events that drive the adenoma-to-carcinoma progression. Because only 5% of the colorectal adenomas progress into carcinomas, there is a strong need to understand the biology of CRC development in order to predict which adenomas will progress and prevent patient over- or under-treatment [7].

The scaffold protein pseudopodium-enriched atypical kinase 1 (PEAK1) associates with integrin adhesion complexes and acts downstream of the epidermal growth factor receptor (EGFR) to coordinate signaling events that control cell proliferation, migration and cytoskeletal remodeling (**chapter 5**) [8, 9]. Integrins are cell adhesion receptors that are known to regulate a diverse array of cellular processes crucial to the formation and progression of solid tumors [10, 11]. In addition, EGFR signaling is an important player in CRC initiation and progression [4]. Because PEAK1 acts downstream of these two receptor families, it could be a potential candidate in the regulation of colorectal adenoma-to-carcinoma progression. In fact, PEAK1 was found to be phosphorylated on Y635, which is a binding site for both Grb2 and tensin-3, in colorectal adenomas but hardly in carcinomas (Beatriz Carvalho, personal correspondence; **chapter 5**). Multiple studies have described increased levels of PEAK1 in human malignancies and showed how PEAK1 promotes disease progression of breast, lung, and pancreatic cancer [9, 12-20]. Yet, in gastric cancer, positive PEAK1 expression is correlated with higher patient survival [21]. Controversy exists as to whether PEAK1 functions as a promoter or suppressor of CRC, as two studies on this subject reported contradicting findings [22, 23].

In this study, we examined the role of PEAK1 in CRC disease progression by deleting PEAK1 in different *in vitro* and *in vivo* models in which lesions are combined that are frequently altered in human patients [4]. Our results indicate that PEAK1, in combination with loss of APC, regulates cell polarity and promotes proliferation of cells stimulated with EGF.

RESULTS

PEAK1 promotes Caco-2 cell proliferation upon EGF stimulation

To determine whether PEAK1 plays a role in CRC development, we first selected different microsatellite stable CRC cell lines with mutations in genes (*APC*, *KRAS*, *BRAF*, *PIK3CA*) that are often found in patients to use as *in vitro* models (Fig. 1A) [4, 24, 25]. Caco-2, SW480, and HT29 PEAK1-deficient cell lines were generated by CRISPR/Cas9 genome editing. For each CRC cell line, we obtained two PEAK1 knockouts that were generated using different guide RNAs (Fig. 1B).

Next, we compared the proliferation of PEAK1-deficient versus wild-type CRC cells (Fig. 1C-E). No significant differences in proliferation were observed between wild-type and PEAK1-deficient cell lines. Because PEAK1 plays a role in EGFR signaling [8], we wondered whether PEAK1 exerts a regulatory effect on EGF-induced cell proliferation. To this end, we repeated the proliferation assays using EGF-supplemented cell culture medium and observed reduced proliferation of PEAK1-deficient Caco-2 cells compared to the wild-type cells (Fig. 1F). For SW480 cells we could observe a small decrease in proliferation of PEAK1-defecient cells for one of the two knockout cell lines (Fig. 1G). There was no significant difference in proliferation of HT29 wild-type versus PEAK1 knockout cells (Fig. 1H). Taken together, PEAK1 can promote CRC cell proliferation, although this requires EGF stimulation and depends on the genetic background of the cells.

PEAK1 contributes to lumen formation of Caco-2 spheroids

Next, we investigated if deletion of PEAK1 also affected cell growth in 3D by growing wild-type and PEAK1-deficient CRC cells as spheroids in Matrigel. For both Caco-2 and SW480 cells we observed reduced size of PEAK1-deficient spheroids after growing the spheroids for 4-7 days in Matrigel (Fig. 2A,B). The HT29 spheroids, both wild-type and PEAK1-deficient, started to disintegrate after 4-7 days of culture in Matrigel and were not taken along in this analysis. To assess whether the spheroid size could be used as a read-out for proliferation, we analyzed the number of cells and morphology of the spheroids by isolating spheroids out of the gel on day 7 and staining the cell nuclei, cell-cell contacts, and actin cytoskeleton. While the SW480 spheroids were composed of a solid mass of cells, the Caco-2 spheroids formed a polarized cell layer surrounding a lumen (Fig. 2C), in line with previous studies [26, 27]. Therefore, the size differences between the SW480 wild-type and PEAK1-deficient spheroids can provide an indication of reduced cell proliferation in 3D upon loss of PEAK1. However, Caco-2 spheroid size might not provide reliable information about the proliferative capacity of wild-type versus PEAK1 knockout cells in 3D due to the formation of the cystlike structures. The reduced size of the PEAK1-deficient Caco-2 spheroids can be the result of reduced cell proliferation and/or impaired lumen formation.

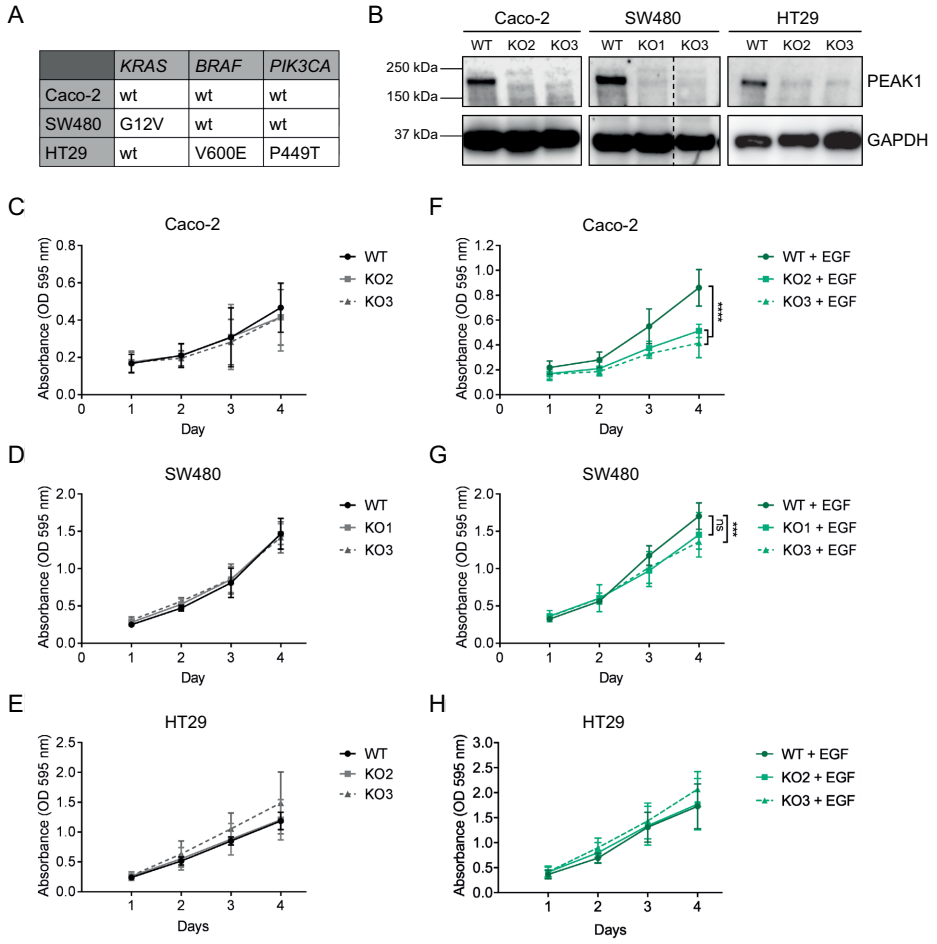

Fig. 1. PEAK1 promotes proliferation of Caco-2 cells stimulated with EGF. (A) Mutation status in CRC critical genes for the selected CRC cell lines. All cell lines contain mutations in *APC* and *TP53*. Adapted from Ahmed *et al., Oncogenesis*. 2013. **(B)** Western blots confirm deletion of PEAK1 in Caco-2, SW480, and HT29 cells that were transfected with CRISPR gRNAs 1-3. The number of the PEAK1 knockout (KO) indicates the gRNA used. GAPDH was used as loading control. **(B-G)** Proliferation assays were performed three times in triplicate. Cells were fixed on the indicated time points, stained with crystal violet, and absorbance was measured at 595 nm. Cell culture medium was supplemented without **(C-E)** or with 50 ng/ml EGF **(F-H)** at day 0. t-test was performed to determine statistical significance. ***, $P < 0.001$. ****, $P < 0.0001$. ns, not significant. Plots show mean with s.d.

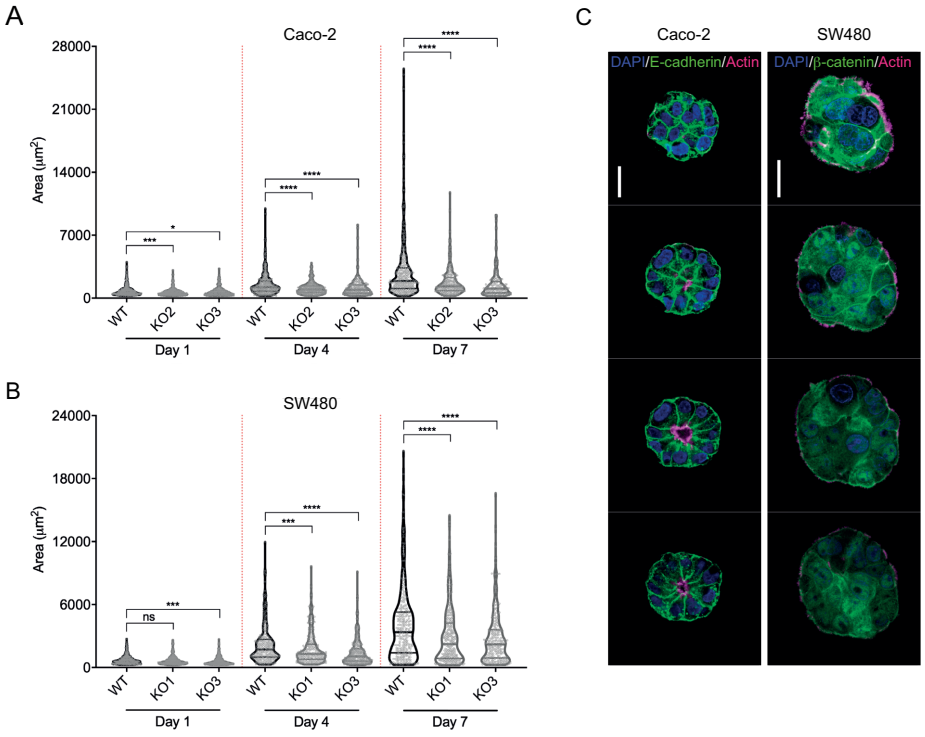

Fig. 2. Decreased size of PEAK1-deficient Caco-2 and SW480 spheroids. (A,B) Caco-2 **(A)** or SW480 **(B)** cells were seeded in Matrigel and imaged on day 1, 4 and 7. Data were obtained from three independent experiments. In total, 300 -330 spheroids analyzed were analysed per condition. Mann-Whitney U-test was used to calculate statistical significance. *P < 0.05; ***P < 0.001; ****P < 0.0001. Violin plots range from the smallest to largest value; lines indicate the median and 25th to 75th percentiles. **(C)** Confocal microscopy z-stack images of spheroids isolated from the Matrigel on day 7, showing E-cadherin (Caco-2) or β-catenin (SW480), actin, and the cell nuclei (stained with DAPI). Scale bar, 20 µm.

To determine whether PEAK1 can play a role in proliferation driven by activated Wnt signaling, we employed genetically engineered mouse models that either express or lack PEAK1 (*Peak1*$^{-/-}$) and in which a tamoxifen-inducible, intestinal epithelium-specific Cre-Recombinase (*VilCreER*^{T2}) excises floxed *Apc* alleles (*Apc*$^{fl/fl}$) to drive proliferation [28, 29]. Intestinal hyperproliferation in the *VilCreER*^{T2}*; Apc*$^{fl/fl}$ and *VilCreER*^{T2}*; Apc*$^{fl/fl}$*; Peak1*$^{-/-}$ mice upon intraperitoneal (IP) injection of tamoxifen was compared by scoring proliferating cells in the small intestinal crypts based on BrdU staining (Fig. 3A,B). No significant differences were observed between the proliferating intestinal crypt cells of the two mouse strains (Fig. 3B,C).

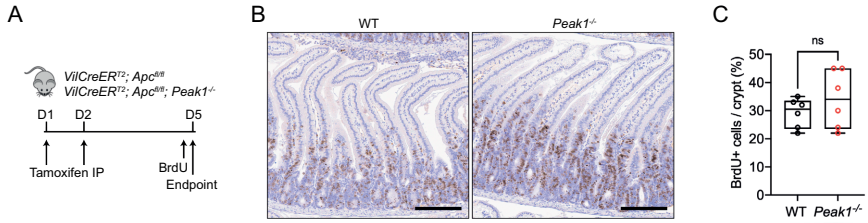

Fig. 3. PEAK1 does not play a role *in vivo* in proliferation driven by loss of Apc. (A) Timeline of the short-term *VilCreER^{T2}; Apc$^{fl/fl}$* mouse models. **(B)** BrdU incorporation in the small intestine of *VilCreER^{T2}; Apc$^{fl/fl}$* (WT) and *VilCreER^{T2}; Apc$^{fl/fl}$; Peak1$^{-/-}$* (*Peak1$^{-/-}$*) mice, visualized by immunohistochemistry. Scale bar, 200 µm. **(C)**. The average percentages of BrdU-positive cells per crypt are shown. Each point represents the average percentage per mouse (n=6 mice per group; at least 25 crypts per sample were scored). Mann-Whitney U test was performed to determine statistical significance. ns, not significant.

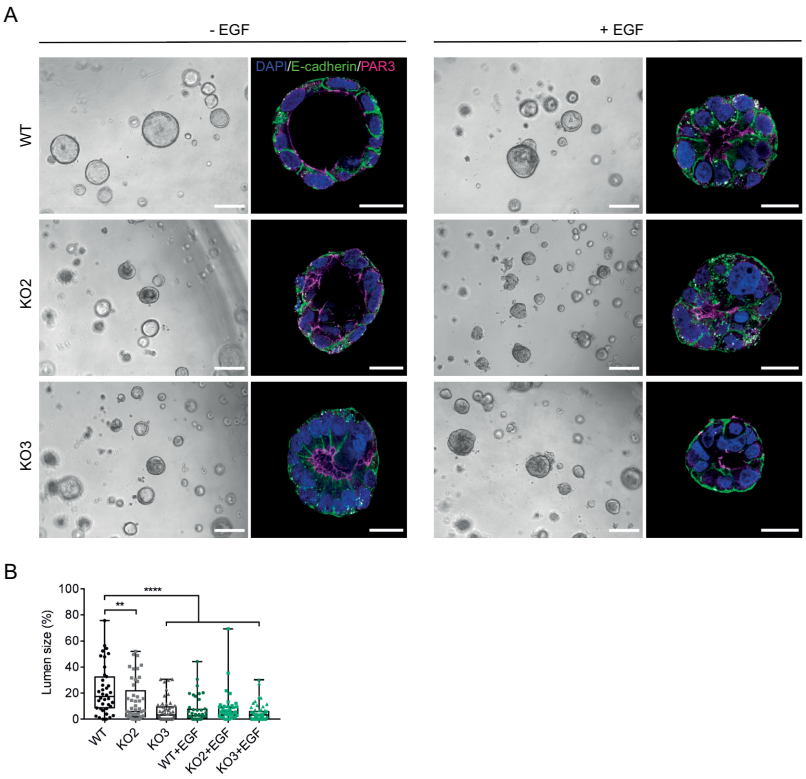

Fig. 4. Lumen size decreased in PEAK1-deficient Caco-2 spheroids. (A) Caco-2 cells were seeded in Matrigel and imaged on day 7 using bright field microscopy (left panels). Scale bar, 200 µm Subsequently, spheroids were isolated from the gels, stained for E-cadherin, PAR3, and the cell nuclei using DAPI, and imaged using confocal microscopy (right panels). Scale bar, 20 µm. Cell culture medium was supplemented with 50 ng/ml EGF as indicated. **(B)**. Quantifications

of the lumen size as a percentage of the total spheroid size. Data were obtained from at least 3 independent experiments. Total number of spheroids analysed: 38 (WT); 50 (KO2); 50 (KO3); 42 (WT+EGF); 38 (KO2+EGF); 53 (KO3+EGF). Box plots range from the 25th to 75th percentile; central line indicates the median; whiskers show smallest to largest value. Mann-Whitney U test was performed to determine statistical significance. **, P < 0.01.****, P < 0.0001.

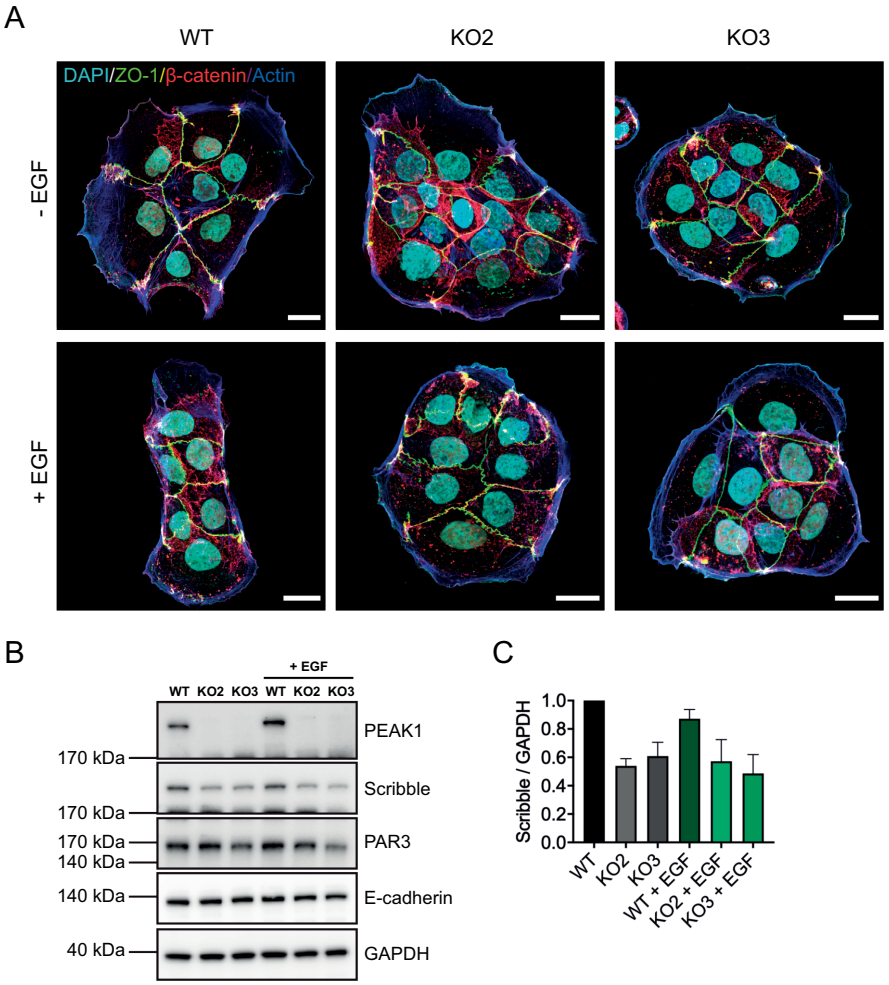

Fig. 5. Scribble expression reduced in PEAK1-deficient Caco-2 cells. (A) Immunofluorescence analysis of cell-cell junctions in Caco-2 cells seeded on coverslips. EGF (50 ng/ml) was added to the cell culture medium as indicated and cells were fixed after 3 days. Scale bar, 20 µm. **(B)** Representative western blots showing the expression of Scribble, PAR3, and E-cadherin in PEAK1 wild-type and deficient Caco-2 cells treated with or without 50 ng/ml EGF for 4 days. GAPDH was used as loading control. **(C)**. Quantifications of Scribble signal intensities normalized to GAPDH levels are shown (n=3 for WT and KO2 samples; n=4 for WT and KO3 samples; bars show mean with s.d.).

To assess whether PEAK1 plays a role in the establishment of apical-basal polarity, we analyzed the ability of Caco-2 wild-type and PEAK1-deficient cells to form lumenized spheroids by isolating the spheroids after 7 days of culture in Matrigel and visualizing cell-cell contacts and the apical surface. We observed reduced lumen formation in PEAK1-deficient Caco-2 spheroids based on staining of PAR3, which forms an apical polarity complex with PAR6 and aPKC [30] (Fig. 4A,B). Upon addition of EGF, all Caco-2 spheroids showed loss of lumen formation (Fig. 4A,B).
No obvious changes were observed in cell morphology and assembly of cell-cell junctions between wild-type and PEAK1-deficient Caco-2 cells seeded on coverslips (Fig. 5A).
To gain more insight into how PEAK1 regulates spheroid lumenization mechanistically, we analyzed the expression of PAR3, E-cadherin, and the apical polarity protein Scribble [31, 32]. Expression of Scribble, but not of PAR3 or E-cadherin, was reduced in the two PEAK1 knockout cell lines, both in untreated and EGF-treated cells (Fig. 5B,C).
In summary, PEAK1 promotes Caco-2 spheroid polarization and lumenization, possibly by regulating the expression of the polarity protein Scribble.

PEAK1 plays no role in tumorigenesis *in vivo*

Finally, we examined the role of PEAK1 in CRC progression by using different CRC mouse models (*VilCreER^{T2}; Apc$^{fl/+}$*, *VilCreER^{T2}; Apc$^{fl/+}$; Kras$^{G12D/+}$*, and *VilCreER^{T2}; Apc$^{fl/+}$; Pten$^{fl/+}$*) that develop spontaneous intestinal tumors upon induction with tamoxifen [28, 29, 33]. Currently, the animal experiments for the *VilCreER^{T2}; Apc$^{fl/+}$* model are still ongoing. The first results of the *VilCreER^{T2}; Apc$^{fl/+}$; Kras$^{G12D/+}$* and *VilCreER^{T2}; Apc$^{fl/+}$; Pten$^{fl/+}$* models show no differences in survival time and tumor burden in the small intestine between PEAK1 wild-type and deficient mice (Fig. 6A-D, Fig, 7A-C), indicating that PEAK1 most likely does not contribute to CRC progression.

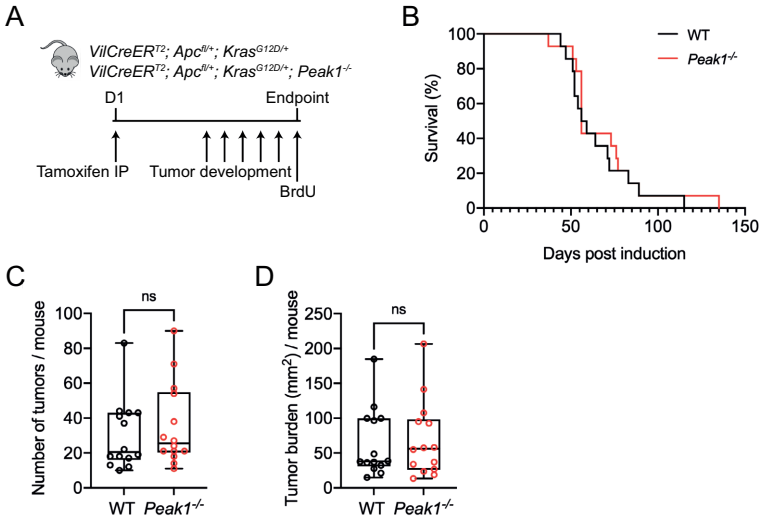

Fig. 6. PEAK1 does not affect Apc-deficient, oncogenic Kras-driven tumorigenesis. (A) Timeline of the long-term *VilCreER^{T2}; Apc$^{fl/+}$; Kras$^{G12D/+}$* mouse models. Mice were injected with tamoxifen and sacrificed when they showed symptoms of intestinal tumors (Endpoint). **(B)** Kaplan-Meier survival plots comparing *VilCreER^{T2}; Apc$^{fl/fl}$; Kras$^{G12D/+}$* (WT) and *VilCreER^{T2}; Apc$^{fl/fl}$; Kras$^{G12D/+}$; Peak1$^{-/-}$* (*Peak1$^{-/-}$*) mice after induction. **(C)**. The number of tumors in the small intestine was scored macroscopically at the endpoint of the experiment. **(D)**. The tumor burden was defined as the sum of the area (πr^2) of all tumors. n=14 mice per group. Mann-Whitney U test was performed to determine statistical significance. ns, not significant.

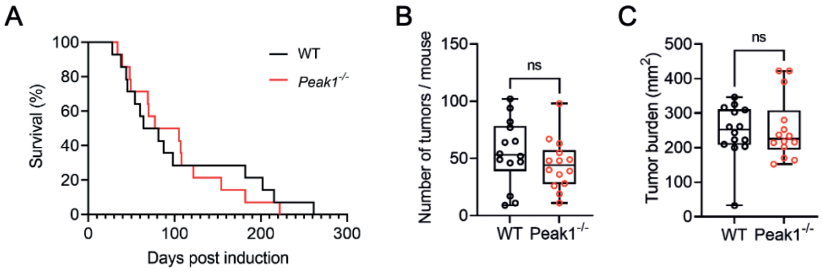

Fig. 7. PEAK1 does not affect tumorigenesis driven by loss of Apc and Pten. (A) Kaplan-Meier survival plots comparing *VilCreER^{T2}; Apc$^{fl/fl}$; Pten$^{fl/+}$* (WT) and *VilCreER^{T2}; Apc$^{fl/fl}$; Pten$^{fl/+}$; Peak1$^{-/-}$* (*Peak1$^{-/-}$*) mice. Animals were injected with tamoxifen and sacrificed when they showed symptoms of intestinal tumors, similar to the mouse model described in Fig. 6. **(B)**. The number of tumors in the small intestine was scored macroscopically at the endpoint of the experiment. **(C)**. The tumor burden was defined as the sum of the area (πr^2) of all tumors. n=14 mice per group. Mann-Whitney U test was performed to determine statistical significance. ns, not significant.

DISCUSSION

In this study, we investigated the role of PEAK1 in the colorectal adenoma-to-carcinoma progression. The results indicate that PEAK1 is not involved in the regulation of intestinal cell proliferation driven by activated Wnt signaling due to loss of APC nor in promoting tumorigenesis driven by oncogenic KRAS or loss of PTEN. However, PEAK1 does promote Caco-2 cell proliferation upon EGF stimulation. In addition, PEAK1 regulates Caco-2 spheroid polarization and lumenization. The obtained results indicate that PEAK1 could be involved in the regulation of colorectal cancer cell proliferation and polarity. However, based on our *in vivo* studies, it does not seem to play a major role in the colorectal adenoma-to-carcinoma progression.

Cell proliferation was decreased in both PEAK1-deficient Caco-2 cell lines treated with EGF, while this effect on proliferation was only minor in SW480 cells and not present in HT29 cells. Preliminary flow cytometry experiments showed that the HT29 cells express the EGFR at higher levels than the Caco-2 cells (data not shown), indicating that the differences in cell proliferation upon EGF stimulation are not caused by differences in expression level of the EGFR. In contrast to the Caco-2 cells, SW480 and HT29 cells harbor oncogenic mutations in the *KRAS* and *BRAF/PIK3CA* genes, respectively (Fig. 1A) [24, 25]. PEAK1 acts downstream of the EGFR and binds the adaptor proteins Shc1 and Grb2 directly (**chapter 5**) [8, 34]. Possibly, PEAK1 could act upstream of KRAS and BRAF and, subsequently, deletion of PEAK1 in the SW480 and HT29 cells might not have a major effect on signaling events downstream of the EGFR that regulate cell proliferation. In contrast to the 2D proliferation assays, PEAK1-deficient SW480 spheroids show reduced growth compared to wild-type spheroids. The proliferation differences observed in 2D versus 3D can be attributed to distinct activation of signaling events [35, 36]. However, PEAK1 does not contribute to tumor incidence and growth in the *VilCreER^{T2}; Apc$^{fl/+}$; Kras$^{G12D/+}$* CRC mouse model and thus does not play a major role in oncogenic KRAS-driven CRC progression. Based on the 2D Caco-2 proliferation assays, PEAK1 might drive EGF-stimulated colorectal adenoma growth. The ongoing animal experiments with the *VilCreER^{T2}; Apc$^{fl/+}$* model will shed light on the role of PEAK1 in this stage of colorectal tumorigenesis.

The potential role of PEAK1 in driving colorectal adenoma growth seems in apparent contrast to its function in regulating Caco-2 spheroid polarization and lumenization. Loss of epithelial polarity is a characteristic of malignant carcinomas [37, 38], which would indicate that PEAK1 might act as a tumor suppressor that establishes and/or maintains apical-basal polarity. However, spheroid lumenization is lost upon treatment with a high (50 ng/ml) EGF concentration, in line with previous studies that demonstrate that EGFR signaling suppresses the formation of apical domains [39, 40]. Further research is needed to understand how PEAK1 would regulate cell polarity. Our data indicates

that the expression of the polarity protein Scribble is partially controlled by PEAK1. Both PEAK1 and Scribble were identified in the proximitome of integrin β1 (**chapter 5**) and as core components of integrin adhesion complexes [41]. Scribble was not found as a direct interactor of PEAK1 but these two proteins could be connected via Shroom2, which is associated with cell-cell junctions, the actin cytoskeleton, and binds both PEAK1 and Scribble (**chapter 5**) [42, 43]. Of interest, a region on the X chromosome (Xp22.2), which appears to be within the distal promoter region of *SHROOM2*, was identified as a CRC risk locus [44]. In addition, other interactions between PEAK1 and components of its interactome might be worth studying in the context of CRC, as the PEAK1-associated proteins MCC, PRAG1 (Sgk223; Pragmin), RASAL2, and ASAP proteins contribute to CRC disease progression [45-51].

So far, we mainly focused on examining the role of PEAK1 in cell proliferation and spheroid/tumor growth. Future studies are required to determine whether PEAK1 could regulate cancer cell invasion/migration and play a role in the formation of invasive carcinomas and metastasis. *In vitro* transwell invasion assays could be performed comparing invasion of wild-type versus PEAK1-deficient SW480 and HT29 cells. Finally, functional studies should be conducted that compare wild-type to PEAK1 knockout and PEAK1-Y635F mutant CRC cell lines to unravel the implications of the differential PEAK1 phosphorylation on Y635 in adenoma formation.

In summary, PEAK1 regulates cellular processes in a cell type-specific and context-dependent manner. PEAK1 might regulate polarity and EGF-induced proliferation in colorectal adenomas that lack APC but do not harbor mutations in the oncogene KRAS or tumor suppressor PTEN. Future studies are required to elucidate whether PEAK1 plays a role in the early formation of colorectal adenomas.

MATERIALS AND METHODS

Antibodies

Primary antibodies used are listed in Table 1. Secondary antibodies were as follows: goat anti-rabbit Alexa Fluor 488, goat anti-mouse Alexa Fluor 568, goat anti-rabbit or anti-mouse Alexa Fluor 647 (Invitrogen), stabilized goat anti-mouse or anti-rabbit HRP-conjugated (Bio-Rad) and rabbit anti-goat HRP-conjugated (Zymax).

Table 1: Primary antibody list

Antibody	Clone	Obtained from	Host	Application
PEAK1	D4G6J	Cell Signaling Technology (#72908)	Rabbit	IF: 1:100 WB: 1:1000
GAPDH	6C5	EMD Millipore (#CB1001)	Mouse	WB: 1:5000
β-catenin		BD Trans. (#610154)	Mouse	IF: 1:100
BrdU		Dako (#M 0744)	Mouse	IHC: 1:100
E-cadherin	36	BD Biosciences	Mouse	IF: 1:100 WB: 1:2000
PAR3	H-70	Santa Cruz (#sc-98509)	Rabbit	IF: 1:50 WB: 1:500
Scribble	C-20	Santa Cruz (#sc-11048)	Goat	WB: 1:500
ZO-1		Zymed (#61-7300)	Rabbit	IF: 1:100

Cell lines

Caco-2, HT29, and SW480 cell lines were kindly provided by Beatriz Carvalho. All cell lines were cultured in Dulbecco's modified Eagle's medium (DMEM) containing 10% heat-inactivated fetal bovine serum and antibiotics and maintained at 37°C in a humidified, 5% CO_2 atmosphere.

Generation of PEAK1-deficient cells

The target gRNAs against human *PEAK1* (exon4; 5'-GTGGGCTTCACAGCTATAGT-3', 5'-TGTGAAGCCCACTATGATAG-3', and 5'-TGCCCGTGTTCCTGATGCGG-3', referred to as gRNA1, gRNA2, and gRNA3, respectively) were cloned into pX330-U6-Chimeric_BB-CBh-hSpCas9 (a kind gift from Feng Zhang [52]; Addgene plasmid #42230). Cells were transfected with this vector using lipofectamine® 2000 (Invitrogen) and selected with 2.5 µg ml^{-1} puromycin for 3 days following transfection.

Western blotting

Cells were washed in cold PBS, lysed in RIPA buffer (20 mM Tris-HCl (pH 7.5), 100 mM NaCl, 4 mM EDTA (pH 7.5), 1% NP-40, 0.1% SDS, 0.5% sodium deoxycholate) supplemented with a protease inhibitor cocktail (Sigma), 1.5 mM Na_3VO_4, and 15 mM NaF (Cell Signaling Technology), and cleared by centrifugation at 14.000 x *g* for 30 min at 4°C. Lysates were mixed with sample buffer (50 mM Tris-HCl pH 6.8, 2% SDS, 10% glycerol, 12.5 mM EDTA, 0.02% bromophenol blue) containing a final concentration of 2% β-mercaptoethanol and denatured at 95°C for 10 min. Proteins were separated by electrophoresis using Bolt Novex 4–12% gradient Bis-Tris (Invitrogen) or homemade 6% polyacrylamide gels, transferred to Immobilon-P transfer membranes (Millipore Corp) and blocked for at

least 30 min in 2% BSA in TBST buffer (10 mM Tris (pH 7.5), 150 mM NaCl, and 0.3% Tween-20). Primary antibody (diluted in 2% BSA in TBST buffer) incubation took place overnight at 4°C. After washing twice with TBST and twice with TBS buffer, blots were incubated for 1 h hour at room temperature with horseradish peroxidase–conjugated secondary antibodies (diluted 1:3.000 in 2% BSA in TBST buffer). After subsequent washing steps, the bound antibodies were detected by enhanced chemiluminescence using Clarity™ Western ECL Substrate (Bio-Rad) as described by the manufacturer. Signal intensities were quantified using ImageJ [53, 54].

Proliferation assays

Cells were seeded in 96-well plate (SW480 and HT29: 10.000 cells/well; Caco-2: 7,500 cells/well) in triplicate. Cells were fixed after 1, 2, 3, or 4 days with 2% paraformaldehyde for 10 min, gently washed 3 times with H_2O and air-dried. Fixed cells were stained with 100 µl of 5 mg/ml crystal violet (dissolved in 2% ethanol) at room temperature on a plate shaker for 10 minutes, rinsed three times with H_2O and then air- dried. Subsequently, the DNA-bound crystal violet was solubilized with 100 µl of 2% SDS in H_2O and its absorbance was measured at 595 nm on a microplate reader (Bio-Rad) using MPM5 software.

Spheroids

Cells (5×10^3 cells/well) were mixed with 2% Matrigel in culture medium and seeded in a 96-wells plate coated with Matrigel (70 µl/well). Images were taken 1, 4 and 7 days after seeding, using a Zeiss Axiovert 200M microscope with an A-Plan 10×/0.25 Ph1 M27 objective. Spheroids were isolated after 7 days, by incubating the gels with 100 µl recovery solution (Corning) for 1 hour at 4°C. The spheroid-containing gels were resuspended and transferred to an Eppendorf tube, washed three times with cold PBS and cleared by centrifugation at 1200 rpm for 3 min at 4°C, spheroid suspensions were placed in a square drawn with Dako (hydrophobic) pen on poly-L-lysine (0.1% w/v in H_2O; ChemCruz)-coated slides and fixed with 4% paraformaldehyde for 10 min. Image analysis was performed using Fiji (ImageJ) [53, 54].

Immunofluorescence

Subconfluent cells were fixed with 2% paraformaldehyde for 10 min, permeabilized with 0.2% Triton-X-100 for 5 min, and blocked with PBS containing 2% BSA (Sigma) for at least 30 min. Next, cells were incubated with the primary antibodies for 1 h at room temperature (for 2D experiments) or overnight at 4°C (for spheroids). Cells were washed three times before incubation with the secondary antibodies for 1 h. Additionally, the nuclei were stained with DAPI and filamentous actin was visualized using Alexa Fluor 488 or 647-conjugated phalloidin (Biolegend; AAT Bioquest). After three washing steps with PBS, the coverslips were mounted onto glass slides in Mowiol. Images were ob-

tained using a Leica TCS SP5 confocal microscope with a 63x (NA 1.4) oil objective (2D experiments) or 63x (NA 1.2) water objective (spheroids).

Animal experiments

All animal studies were performed according to the Dutch guidelines for care and use of laboratory animals and were approved by the animal welfare committee of the Netherlands Cancer Institute.

The (conditional) PEAK1 knockout mice were generated using CRISPR/Cas9 genome editing by pronuclear microinjection of 50 ng/µl *in vitro* transcribed Cas9 mRNA, 25 ng/µl gRNAs targeting the *Peak1* intronic regions flanking exons 4-7 (5'-GGGATTGATTTTTAGCGCACTGG-3' and 5'-TGCTATATGAGTAGCCACTCTGG-3') and two single-stranded oligodeoxynucleotides repair templates containing the *loxP* site (5'-ATAACTTCGTATAGCATACATTATACGAAGTTAT-3') flanked by 60 bp homology arms (Integrated DNA Technologies). After backcrossing to the FVB/N background, mice were obtained with a floxed *Peak1* allele ($Peak1^{+/fl}$) and complete deletion ($Peak1^{+/-}$). After at least 4 backcrosses to FVB/N background, the heterozygous $Peak^{+/-}$ mice were intercrossed to obtain homozygous $Peak1^{-/-}$ mice. The genotypes were analyzed by PCR on genomic DNA using the following primers: P1: 5'-CCCGGGTTTGCCTTTGATAC-3', P2: 5'-GCCTGGCGATGGCAAGAATA-3', and P3: 5'-CCATCTCCTCTAGCTGACCCTT-3'. In one PCR reaction, primers P1 and P2 were combined to detect a WT band (218 bp) and P2 and P3 were combined to detect a KO band (189 bp).

No embryonic lethality or pathological alterations related to the genotype were observed in $Peak1^{-/-}$ mice. These mice were intercrossed with $VilCreER^{T2}$; $Apc^{fl/fl}$; $Kras^{G12D/+}$ or *VilCreERT2*; $Apc^{fl/+}$; $Pten^{fl/+}$ (kindly provided by William Faller) to obtain the strains described in the figures. The animals were kept in a pathogen-free, temperature-controlled environment with a 12 h dark / 12 h light cycle. Mice received standard chow and acidified water *ad libitum*. Roughly equal numbers of male and female animals were used. Male and female mice were housed separately, and 2–5 mice were housed per cage. Mice used for experiments were of mixed FVB/N - C57BL/6J background.

Sample size calculations were performed using two-sample t test, powered to detect a mean difference of 30% at a power of 0.85 to a p-value of 0.05 assuming a 25% group standard deviation using a Java Applet for Power and Sample Size (Lenth, R. V. (2006-9). Retrieved March 2020, from http://www.stat.uiowa.edu/~rlenth/Power). For short-term studies to analyze hyperproliferation of the intestinal epithelium, 6 animals per group were used. For long-term studies of spontaneous tumor development, 14 animals per group were used.

All animals were injected intraperitoneally with 80 mg/kg of tamoxifen dissolved in sunflower oil on day 1 to induce Cre-Lox recombination. For tumor studies, animals were monitored 2-3 times a week until they showed signs of tumor formation, which

included weight loss, hunching, paling feet from anaemia, and/or development of a prolapse. Animals were injected intraperitoneally with 50 mg/kg BrdU 2h before dissection. Tumors were scored macroscopically by counting the numbers of visible tumors after fixation of the opened intestinal tissue in ethanol glacial acetic acid mixture (3:1), containing 2% of formaldehyde (EAF).
For short-term experiments, animals were injected with a second dose of tamoxifen on day 2 and BrdU on day 5, 2h before dissection. Intestinal tissues were fixed in EAF, embedded in paraffin, and BrdU was visualized by immunohistochemistry. Images were taking on an Aperio ScanScope, using ImageScope software version 12.0.0 (Aperio). No randomization was used and researchers were blinded to genotypes during the macroscopical tumor scoring and counting of the BrdU-positive cells per crypt.

Statistical analysis

Mann-Whitney U or t-test (two-tailed P value) was performed using GraphPad Prism (version 9). In figures, statistically significant values are shown as *P < 0.05; **P < 0.01; ***P < 0.001; ****P < 0.0001. Graphs were made in GraphPad Prism and show all data points.

ACKNOWLEDGEMENTS

We would like to acknowledge Beatriz Carvalho for helpful discussions and for sharing cell lines. We further would like to thank William Faller and Rob van der Kammen for providing mouse strains and assistance with the animal experiments and the NKI animal facility for support. This work was supported by the Dutch Cancer Society (project 12143).

REFERENCES

1. Siegel, R.L., K.D. Miller, A. Goding Sauer, S.A. Fedewa, L.F. Butterly, J.C. Anderson, A. Cercek, R.A. Smith, and A. Jemal, *Colorectal cancer statistics, 2020.* CA Cancer J Clin, 2020. **70**(3): p. 145-164.
2. Siegel, R.L., K.D. Miller, and A. Jemal, *Cancer statistics, 2020.* CA Cancer J Clin, 2020. **70**(1): p. 7-30.
3. Ferlay, J., M. Colombet, I. Soerjomataram, T. Dyba, G. Randi, M. Bettio, A. Gavin, O. Visser, and F. Bray, *Cancer incidence and mortality patterns in Europe: Estimates for 40 countries and 25 major cancers in 2018.* Eur J Cancer, 2018. **103**: p. 356-387.
4. Markowitz, S.D. and M.M. Bertagnolli, *Molecular origins of cancer: Molecular basis of colorectal cancer.* N Engl J Med, 2009. **361**(25): p. 2449-60.
5. Vogelstein, B., E.R. Fearon, S.R. Hamilton, S.E. Kern, A.C. Preisinger, M. Leppert, Y. Nakamura, R. White, A.M. Smits, and J.L. Bos, *Genetic alterations during colorectal-tumor development.* N Engl J Med, 1988. **319**(9): p. 525-32.
6. Fearon, E.R. and B. Vogelstein, *A genetic model for colorectal tumorigenesis.* Cell, 1990. **61**(5): p. 759-67.
7. Sillars-Hardebol, A.H., B. Carvalho, M. van Engeland, R.J. Fijneman, and G.A. Meijer, *The adenoma hunt in colorectal cancer screening: defining the target.* J Pathol, 2012. **226**(1): p. 1-6.
8. Zheng, Y., C. Zhang, D.R. Croucher, M.A. Soliman, N. St-Denis, A. Pasculescu, L. Taylor, S.A. Tate, W.R. Hardy, K. Colwill, A.Y. Dai, R. Bagshaw, J.W. Dennis, A.C. Gingras, R.J. Daly, and T. Pawson, *Temporal regulation of EGF signalling networks by the scaffold protein Shc1.* Nature, 2013. **499**(7457): p. 166-71.
9. Wang, Y., J.A. Kelber, H.S. Tran Cao, G.T. Cantin, R. Lin, W. Wang, S. Kaushal, J.M. Bristow, T.S. Edgington, R.M. Hoffman, M. Bouvet, J.R. Yates, 3rd, and R.L. Klemke, *Pseudopodium-enriched atypical kinase 1 regulates the cytoskeleton and cancer progression [corrected].* Proc Natl Acad Sci U S A, 2010. **107**(24): p. 10920-5.
10. Desgrosellier, J.S. and D.A. Cheresh, *Integrins in cancer: biological implications and therapeutic opportunities.* Nat Rev Cancer, 2010. **10**(1): p. 9-22.
11. Hamidi, H. and J. Ivaska, *Every step of the way: integrins in cancer progression and metastasis.* Nat Rev Cancer, 2018. **18**(9): p. 533-548.
12. Ding, C., W. Tang, X. Fan, X. Wang, H. Wu, H. Xu, W. Xu, W. Gao, and G. Wu, *Overexpression of PEAK1 contributes to epithelial-mesenchymal transition and tumor metastasis in lung cancer through modulating ERK1/2 and JAK2 signaling.* Cell Death Dis, 2018. **9**(8): p. 802.
13. Kelber, J.A., T. Reno, S. Kaushal, C. Metildi, T. Wright, K. Stoletov, J.M. Weems, F.D. Park, E. Mose, Y. Wang, R.M. Hoffman, A.M. Lowy, M. Bouvet, and R.L. Klemke, *KRas induces a Src/PEAK1/ErbB2 kinase amplification loop that drives metastatic growth and therapy resistance in pancreatic cancer.* Cancer Res, 2012. **72**(10): p. 2554-64.
14. Fujimura, K., T. Wright, J. Strnadel, S. Kaushal, C. Metildi, A.M. Lowy, M. Bouvet, J.A. Kelber, and R.L. Klemke, *A hypusine-eIF5A-PEAK1 switch regulates the pathogenesis of pancreatic cancer.* Cancer Res, 2014. **74**(22): p. 6671-81.
15. Strnadel, J., S. Choi, K. Fujimura, H. Wang, W. Zhang, M. Wyse, T. Wright, E. Gross, C. Peinado, H.W. Park, J. Bui, J. Kelber, M. Bouvet, K.L. Guan, and R.L. Klemke, *eIF5A-PEAK1 Signaling Regulates YAP1/TAZ Protein Expression and Pancreatic Cancer Cell Growth.* Cancer Res, 2017. **77**(8): p. 1997-2007.

16. Croucher, D.R., F. Hochgrafe, L. Zhang, L. Liu, R.J. Lyons, D. Rickwood, C.M. Tactacan, B.C. Browne, N. Ali, H. Chan, R. Shearer, D. Gallego-Ortega, D.N. Saunders, A. Swarbrick, and R.J. Daly, *Involvement of Lyn and the atypical kinase SgK269/PEAK1 in a basal breast cancer signaling pathway.* Cancer Res, 2013. **73**(6): p. 1969-80.
17. Agajanian, M., A. Campeau, M. Hoover, A. Hou, D. Brambilla, S.L. Kim, R.L. Klemke, and J.A. Kelber, *PEAK1 Acts as a Molecular Switch to Regulate Context-Dependent TGFbeta Responses in Breast Cancer.* PLoS One, 2015. **10**(8): p. e0135748.
18. Abu-Thuraia, A., M.A. Goyette, J. Boulais, C. Delliaux, C. Apcher, C. Schott, R. Chidiac, H. Bagci, M.P. Thibault, D. Davidson, M. Ferron, A. Veillette, R.J. Daly, A.C. Gingras, J.P. Gratton, and J.F. Cote, *AXL confers cell migration and invasion by hijacking a PEAK1-regulated focal adhesion protein network.* Nat Commun, 2020. **11**(1): p. 3586.
19. Runa, F., Y. Adamian, and J.A. Kelber, *Ascending the PEAK1 toward targeting TGFbeta during cancer progression: Recent advances and future perspectives.* Cancer Cell Microenviron, 2016. **3**(1).
20. Hamalian, S., R. Guth, F. Runa, F. Sanchez, E. Vickers, M. Agajanian, J. Molnar, T. Nguyen, J. Gamez, J.D. Humphries, A. Nayak, M.J. Humphries, J. Tchou, I.K. Zervantonakis, and J.A. Kelber, *A SNAI2-PEAK1-INHBA stromal axis drives progression and lapatinib resistance in HER2-positive breast cancer by supporting subpopulations of tumor cells positive for antiapoptotic and stress signaling markers.* Oncogene, 2021.
21. Guo, Q., W. Qin, B. Li, H. Yang, J. Guan, Z. Liu, and S. Li, *Analysis of a cytoskeleton-associated kinase PEAK1 and E-cadherin in gastric cancer.* Pathol Res Pract, 2014. **210**(12): p. 793-8.
22. Ding, C., W. Tang, H. Wu, X. Fan, J. Luo, J. Feng, K. Wen, and G. Wu, *The PEAK1-PPP1R12B axis inhibits tumor growth and metastasis by regulating Grb2/PI3K/Akt signalling in colorectal cancer.* Cancer Lett, 2019. **442**: p. 383-395.
23. Huang, L., C. Wen, X. Yang, Q. Lou, X. Wang, J. Che, J. Chen, Z. Yang, X. Wu, M. Huang, P. Lan, L. Wang, A. Iwamoto, J. Wang, and H. Liu, *PEAK1, acting as a tumor promoter in colorectal cancer, is regulated by the EGFR/KRas signaling axis and miR-181d.* Cell Death Dis, 2018. **9**(3): p. 271.
24. Ahmed, D., P.W. Eide, I.A. Eilertsen, S.A. Danielsen, M. Eknaes, M. Hektoen, G.E. Lind, and R.A. Lothe, *Epigenetic and genetic features of 24 colon cancer cell lines.* Oncogenesis, 2013. **2**: p. e71.
25. Berg, K.C.G., P.W. Eide, I.A. Eilertsen, B. Johannessen, J. Bruun, S.A. Danielsen, M. Bjornslett, L.A. Meza-Zepeda, M. Eknaes, G.E. Lind, O. Myklebost, R.I. Skotheim, A. Sveen, and R.A. Lothe, *Multi-omics of 34 colorectal cancer cell lines - a resource for biomedical studies.* Mol Cancer, 2017. **16**(1): p. 116.
26. Jaffe, A.B., N. Kaji, J. Durgan, and A. Hall, *Cdc42 controls spindle orientation to position the apical surface during epithelial morphogenesis.* J Cell Biol, 2008. **183**(4): p. 625-33.
27. Magudia, K., A. Lahoz, and A. Hall, *K-Ras and B-Raf oncogenes inhibit colon epithelial polarity establishment through up-regulation of c-myc.* J Cell Biol, 2012. **198**(2): p. 185-94.

28. Knight, J.R.P., C. Alexandrou, G.L. Skalka, N. Vlahov, K. Pennel, L. Officer, A. Teodosio, G. Kanellos, D.M. Gay, S. May-Wilson, E.M. Smith, A.K. Najumudeen, K. Gilroy, R.A. Ridgway, D.J. Flanagan, R.C.L. Smith, L. McDonald, C. MacKay, A. Cheasty, K. McArthur, E. Stanway, J.D. Leach, R. Jackstadt, J.A. Waldron, A.D. Campbell, G. Vlachogiannis, N. Valeri, K.M. Haigis, N. Sonenberg, C.G. Proud, N.P. Jones, M.E. Swarbrick, H.J. McKinnon, W.J. Faller, J. Le Quesne, J. Edwards, A.E. Willis, M. Bushell, and O.J. Sansom, *MNK Inhibition Sensitizes KRAS-Mutant Colorectal Cancer to mTORC1 Inhibition by Reducing eIF4E Phosphorylation and c-MYC Expression.* Cancer Discov, 2021. **11**(5): p. 1228-1247.
29. Shibata, H., K. Toyama, H. Shioya, M. Ito, M. Hirota, S. Hasegawa, H. Matsumoto, H. Takano, T. Akiyama, K. Toyoshima, R. Kanamaru, Y. Kanegae, I. Saito, Y. Nakamura, K. Shiba, and T. Noda, *Rapid colorectal adenoma formation initiated by conditional targeting of the Apc gene.* Science, 1997. **278**(5335): p. 120-3.
30. Ohno, S., *Intercellular junctions and cellular polarity: the PAR-aPKC complex, a conserved core cassette playing fundamental roles in cell polarity.* Curr Opin Cell Biol, 2001. **13**(5): p. 641-8.
31. Assemat, E., E. Bazellieres, E. Pallesi-Pocachard, A. Le Bivic, and D. Massey-Harroche, *Polarity complex proteins.* Biochim Biophys Acta, 2008. **1778**(3): p. 614-30.
32. Bonello, T.T. and M. Peifer, *Scribble: A master scaffold in polarity, adhesion, synaptogenesis, and proliferation.* J Cell Biol, 2019. **218**(3): p. 742-756.
33. Davies, E.J., V. Marsh Durban, V. Meniel, G.T. Williams, and A.R. Clarke, *PTEN loss and KRAS activation leads to the formation of serrated adenomas and metastatic carcinoma in the mouse intestine.* J Pathol, 2014. **233**(1): p. 27-38.
34. Krasinskas, A.M., *EGFR Signaling in Colorectal Carcinoma.* Patholog Res Int, 2011. **2011**: p. 932932.
35. Riedl, A., M. Schlederer, K. Pudelko, M. Stadler, S. Walter, D. Unterleuthner, C. Unger, N. Kramer, M. Hengstschlager, L. Kenner, D. Pfeiffer, G. Krupitza, and H. Dolznig, *Comparison of cancer cells in 2D vs 3D culture reveals differences in AKT-mTOR-S6K signaling and drug responses.* J Cell Sci, 2017. **130**(1): p. 203-218.
36. Pickl, M. and C.H. Ries, *Comparison of 3D and 2D tumor models reveals enhanced HER2 activation in 3D associated with an increased response to trastuzumab.* Oncogene, 2009. **28**(3): p. 461-8.
37. Wodarz, A. and I. Nathke, *Cell polarity in development and cancer.* Nat Cell Biol, 2007. **9**(9): p. 1016-24.
38. Lee, M. and V. Vasioukhin, *Cell polarity and cancer--cell and tissue polarity as a non-canonical tumor suppressor.* J Cell Sci, 2008. **121**(Pt 8): p. 1141-50.
39. Castanieto, A., M.J. Johnston, and T.G. Nystul, *EGFR signaling promotes self-renewal through the establishment of cell polarity in Drosophila follicle stem cells.* Elife, 2014. **3**.
40. Lof-Ohlin, Z.M., P. Nyeng, M.E. Bechard, K. Hess, E. Bankaitis, T.U. Greiner, J. Ameri, C.V. Wright, and H. Semb, *EGFR signalling controls cellular fate and pancreatic organogenesis by regulating apicobasal polarity.* Nat Cell Biol, 2017. **19**(11): p. 1313-1325.
41. Chastney, M.R., C. Lawless, J.D. Humphries, S. Warwood, M.C. Jones, D. Knight, C. Jorgensen, and M.J. Humphries, *Topological features of integrin adhesion complexes revealed by multiplexed proximity biotinylation.* J Cell Biol, 2020. **219**(8).

42. Amano, M., T. Hamaguchi, M.H. Shohag, K. Kozawa, K. Kato, X. Zhang, Y. Yura, Y. Matsuura, C. Kataoka, T. Nishioka, and K. Kaibuchi, *Kinase-interacting substrate screening is a novel method to identify kinase substrates.* J Cell Biol, 2015. **209**(6): p. 895-912.
43. Hildebrand, J.D. and P. Soriano, *Shroom, a PDZ domain-containing actin-binding protein, is required for neural tube morphogenesis in mice.* Cell, 1999. **99**(5): p. 485-97.
44. Dunlop, M.G., S.E. Dobbins, S.M. Farrington, A.M. Jones, C. Palles, N. Whiffin, A. Tenesa, S. Spain, P. Broderick, L.Y. Ooi, E. Domingo, C. Smillie, M. Henrion, M. Frampton, L. Martin, G. Grimes, M. Gorman, C. Semple, Y.P. Ma, E. Barclay, J. Prendergast, J.B. Cazier, B. Olver, S. Penegar, S. Lubbe, I. Chander, L.G. Carvajal-Carmona, S. Ballereau, A. Lloyd, J. Vijayakrishnan, L. Zgaga, I. Rudan, E. Theodoratou, C. Colorectal Tumour Gene Identification, J.M. Starr, I. Deary, I. Kirac, D. Kovacevic, L.A. Aaltonen, L. Renkonen-Sinisalo, J.P. Mecklin, K. Matsuda, Y. Nakamura, Y. Okada, S. Gallinger, D.J. Duggan, D. Conti, P. Newcomb, J. Hopper, M.A. Jenkins, F. Schumacher, G. Casey, D. Easton, M. Shah, P. Pharoah, A. Lindblom, T. Liu, G. Swedish Low-Risk Colorectal Cancer Study, C.G. Smith, H. West, J.P. Cheadle, C.C. Group, R. Midgley, D.J. Kerr, H. Campbell, I.P. Tomlinson, and R.S. Houlston, *Common variation near CDKN1A, POLD3 and SHROOM2 influences colorectal cancer risk.* Nat Genet, 2012. **44**(7): p. 770-6.
45. Pan, Y., J.H.M. Tong, R.W.M. Lung, W. Kang, J.S.H. Kwan, W.P. Chak, K.Y. Tin, L.Y. Chung, F. Wu, S.S.M. Ng, T.W.C. Mak, J. Yu, K.W. Lo, A.W.H. Chan, and K.F. To, *RASAL2 promotes tumor progression through LATS2/YAP1 axis of hippo signaling pathway in colorectal cancer.* Mol Cancer, 2018. **17**(1): p. 102.
46. Lecointre, C., V. Simon, C. Kerneur, F. Allemand, A. Fournet, I. Montarras, J.L. Pons, M. Gelin, C. Brignatz, S. Urbach, G. Labesse, and S. Roche, *Dimerization of the Pragmin Pseudo-Kinase Regulates Protein Tyrosine Phosphorylation.* Structure, 2018. **26**(4): p. 545-554 e4.
47. Leroy, C., C. Fialin, A. Sirvent, V. Simon, S. Urbach, J. Poncet, B. Robert, P. Jouin, and S. Roche, *Quantitative phosphoproteomics reveals a cluster of tyrosine kinases that mediates SRC invasive activity in advanced colon carcinoma cells.* Cancer Res, 2009. **69**(6): p. 2279-86.
48. Roche, S., C. Lecointre, V. Simon, and G. Labesse, *SHEDding light on the role of Pragmin pseudo-kinases in cancer.* Am J Cancer Res, 2019. **9**(2): p. 449-454.
49. Muller, T., U. Stein, A. Poletti, L. Garzia, M. Rothley, D. Plaumann, W. Thiele, M. Bauer, A. Galasso, P. Schlag, M. Pankratz, M. Zollo, and J.P. Sleeman, *ASAP1 promotes tumor cell motility and invasiveness, stimulates metastasis formation in vivo, and correlates with poor survival in colorectal cancer patients.* Oncogene, 2010. **29**(16): p. 2393-403.
50. Tian, H., J. Qian, L. Ai, Y. Li, W. Su, X.M. Kong, J. Xu, and J.Y. Fang, *Upregulation of ASAP3 contributes to colorectal carcinogenesis and indicates poor survival outcome.* Cancer Sci, 2017. **108**(8): p. 1544-1555.
51. Kinzler, K.W., M.C. Nilbert, B. Vogelstein, T.M. Bryan, D.B. Levy, K.J. Smith, A.C. Preisinger, S.R. Hamilton, P. Hedge, A. Markham, and et al., *Identification of a gene located at chromosome 5q21 that is mutated in colorectal cancers.* Science, 1991. **251**(4999): p. 1366-70.
52. Cong, L., F.A. Ran, D. Cox, S. Lin, R. Barretto, N. Habib, P.D. Hsu, X. Wu, W. Jiang, L.A. Marraffini, and F. Zhang, *Multiplex genome engineering using CRISPR/Cas systems.* Science, 2013. **339**(6121): p. 819-23.

53. Schindelin, J., I. Arganda-Carreras, E. Frise, V. Kaynig, M. Longair, T. Pietzsch, S. Preibisch, C. Rueden, S. Saalfeld, B. Schmid, J.Y. Tinevez, D.J. White, V. Hartenstein, K. Eliceiri, P. Tomancak, and A. Cardona, *Fiji: an open-source platform for biological-image analysis.* Nat Methods, 2012. **9**(7): p. 676-82.
54. Schneider, C.A., W.S. Rasband, and K.W. Eliceiri, *NIH Image to ImageJ: 25 years of image analysis.* Nat Methods, 2012. **9**(7): p. 671-5.